31st Annual International Conference of the IEEE EMBS
Minneapolis, Minnesota, USA, September 2-6, 2009

Simulation of Erythrocyte Deformation in a High Shear Flow

Masanori Nakamura, Sadao Bessho, and Shigeo Wada

Abstract— **Deformation of a red blood cell (RBC) in a high-shear flow was investigated. The RBC was modeled as a closed shell membrane consisting of spring networks in the framework of the energy minimum concept. The simulation of RBC in a parallel shear flow showed deformation parameters of RBC were well agreed with experimental results. The simulation of RBC behavior in various flow fields demonstrated that the shape was determined not only by instantaneous fluid force acting on it but also its deformation history. No consistency was found between the maximum of the first principal strain and conventionally used hemolysis index. Those results addressed the importance of considering an RBC deformation for accurately predicting hemolysis.**

I. Introduction

A red blood cell (RBC) plays an important role in delivering oxygen to body tissues and removing carbon dioxide from them.

An RBC has no nucleus and its membrane is rich in elasticity such that it can pass through a capillary whose diameter is smaller than an RBC. Under physiological conditions, an RBC has a biconcave shape. However, while flowing, it deforms into various shapes by interactions with surrounding fluid. When the deformation becomes excessive, hemolysis, the breaking open of RBC, can occur.

Hemolysis is unwanted phenomena in medical devices. Although hemolytic anemia is no longer critical in most of medical devices, it is reported that plasma free hemoglobin released by the destruction of RBC represents severe pathological conditions in vital organ systems [1]. Hemoglobin scavenges nitric oxide that is a regulator of smooth muscle tone and platelet activations. Depletion of nitric oxide contributes to clinical morbidities, including esophageal spasm, abdominal pain, erectile dysfunction, and thrombosis [2, 3].

Recently, efforts have been made to estimate hemolysis from a flow field of interest by computer simulations [4, 5]. Mechanical damage of RBCs is modeled with shear stress and exposure time based on the experimental data [6] Although a good correlation was found between the proposed hemolysis index and the amount of hemoglobin in a simple flow condition, the index does not reflect the amount of hemolysis as a flow field of interest becomes more complex [5]. One of the reasons for this inconsistency was because the experiment to derive an empirical formula to relate shear stress to hemolysis adopted a viscometer to apply shear stress on RBCs, which provided only one-directional laminar flow. The other reason we postulate is because those predictive methods treated an RBC as a mass point and did not well considered motion and deformation of individual RBCs in a given flow field.

In the present study, we develop an elastic RBC model that can express its motion and deformation behaviors in a high-shear flow. First, RBC behavior in parallel shear flows was simulated for corroborating the RBC model. Second, RBC in a back-step flow was simulated in order to see how the RBC deforms in such a complex flow field and to demonstrate that conventional haemolysis index does not reflect the degree of RBC deformation.

II. Method

A. Modeling of RBC [7]

The RBC membrane is a lipid bilayer reinforced with its underlying structure of cytoskeleton called spectrin. The spectrin network is anchored firmly to the RBC membrane via various trans-membrane proteins, bringing about a high resistance against shear deformation (in-plane deformation). The lipid bilayer has a high fluidity and is relatively less contributive to the shear deformation. Nevertheless, because the number of lipids on the RBC surface is constant, the lipid bilayer offers resistance to membrane area change. Moreover, because both lipid bilayer and spectrin networks have thickness, they resist bending. Therefore, the mechanical nature of the RBC membrane is expressed by fluidic lipid bilayer and elastic spectrin network in a mutually complementary manner [8]. Although it is possible that the lipid bilayer tears off from the spectrin in special cases [9], we here assume that they always deform together (no tearing).

We represent mechanical natures of the RBC membrane by a spring network. As shown in Fig. 1 (a), an RBC at natural state is expressed as a sphere with the diameter of 6.5 μm and the membrane is expressed by a closed shell consisting of triangular meshes. Figure 1 (b) schematically represents a magnified view of two neighboring meshes, showing neighboring meshes are connected with bending springs to

Manuscript received April 7, 2009. This work was supported in part by Grant-in-Aid for Young Scientists (A) 19680024 and gCOE Program "A center of excellence for in silico medicine-oriented worldwide open platform".

M. Nakamura is with Center for Advanced Medical Engineering and Informatics, Osaka University, Toyonaka, Osaka 560-8531 Japan (phone: +81-6-6850-6183; fax: +81-6-6850-6172; e-mail: masanori@me.es.osaka-u.ac.jp).

S. Bessho, was with Graduate School of Engineering Science, Osaka University, Toyonaka, Osaka 560-8531 Japan (e-mail: bessyo@tekka.me.es.osaka-u.ac.jp).

S. Wada is with the Graduate School of Engineering Science, Osaka University, Toyonaka, Osaka 560-8531 Japan (e-mail: shigeo@me.es.osaka-u.ac.jp).

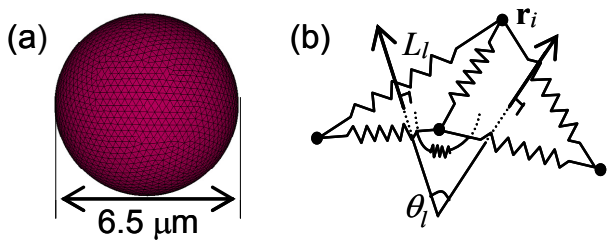

Fig. 1 (a) RBC model, (b) Schematic representation of a mechanical model of RBC membrane

prevent folding of membrane while nodal points are linked by spring elements to resist to stretching. Owing to deformation, elastic energies are generated and stored in RBC. Based on the Hooke's law, we modeled the stretching energy W_s as

$$W_s = \frac{1}{2} k_s \sum_{l=1}^{N} (L_l - L_{l0})^2 \tag{1}$$

where k_s is a spring constant for stretching, N is the number of nodes, L_{l0},L_l are length of spring at the natural state and after deformation. Similarly, the bending energy W_b is modeled

$$W_b = \frac{1}{2} k_b \sum_{l=1}^{N_l} L_l \tan^2\left(\frac{\theta_l}{2}\right) \tag{2}$$

where k_b is a spring constant for bending, N_l is the number of a combination of neighboring meshes and θ_l is the contacting angle between neighboring elements.

The resistance to the membrane area changes is classified into the one to an area change of the whole membrane and the one to an area change of a local element. The former corresponds to the situation where lipid molecules can move freely over the cytoskeletal membrane, while the latter corresponds to the situation where movement of lipid molecules is confined to a local element. Because the lipid bilayer has high fluidity, the former is considered to be predominant [10]. Meanwhile it would be possible that movement of lipid molecules is restricted locally since movement of trans-membrane proteins is somehow restricted by anchoring of the lipid bilayer to the spectrin. Thus, we here model both resistances.

The elastic energy generated by the whole membrane area change is expressed by an energy-like function W_A. Mathematically, it is defined as

$$W_A = \frac{1}{2} k_A \left(\frac{A - A_0}{A_0}\right)^2 A_0 \tag{3}$$

where A_0 and A are the area of the whole membrane at a natural state and after deformation, k_A is a coefficient for whole area constraint. Similarly, the elastic energy generated by a local area change is

$$W_a = \frac{1}{2} k_a \sum_{e=1}^{N_e} \left(\frac{A_e - A_{e0}}{\mathrm{A_{e0}}}\right)^2 A_{e0} \tag{4}$$

where k_a is a coefficient for a local area constraint, N_e is the number of elements consisting of RBC membrane, and A_{e0} and A_e are the area of element e at a natural state and after deformation.

With those modeling, it is possible to determine the RBC shape by defining RBC volume V encapsulated by RBC membrane. By vector analyses, it is possible to rewrite energies (1)-(4) as a function of the positional vector of nodal points $\mathbf{r}_i$. Therefore, the problem to determine the RBC shape is equivalent to calculating positional vectors of nodal points which minimizes the total elastic energy under the constraint that the RBC volume V is equal to V_0;

$$\text{Minimize } W \text{ with respect to } \mathbf{r}_i$$
$$W = W_s + W_b + W_A + W_a \tag{5}$$
$$\text{subject to } V = V_0 .$$

We then introduce an energy-like function for the volume V

$$W_V = \frac{1}{2} k_V \left(\frac{V - V_0}{V_0}\right)^2 V_0 \tag{6}.$$

Including eq. (6) in eq. (5), we rewrite eq. (5) as

$$\text{Minimize } W \text{ with respect to } \mathbf{r}_i$$
$$W = W_s + W_b + W_A + W_a + W_V \tag{7}.$$

B. Modeling of Fluid Forces

While flowing, fluid forces act on an RBC externally from plasma and internally from hemoglobin due to a difference in the velocity between an RBC and fluid flow. Although it is ideal to calculate flow inside and outside an RBC of interest by means of strong coupling of an RBC motion and fluid, it is computationally expensive and unrealistic if we consider surface irregularities and spectrin networks which may influence flow. For simplicity, we here assume that an RBC does not disturb surrounding flow and implement one-way coupling for flow-RBC where flow is pre-defined.

An external fluid force $\mathbf{f}_e^{out}$ acting on element e is resolved into that in a tangential direction $\mathbf{f}_{e,t}^{out}$ and that in a normal direction $\mathbf{f}_{e,n}^{out}$. From Newton's viscosity law and conservation of the fluid momentum, the external forces were modeled as

$$\mathbf{f}_{e,n}^{out} = \rho Q \Delta \mathbf{u}_{\mathbf{n}}^{\mathbf{e}}, \tag{8}$$

$$\mathbf{f}_{e,t}^{out} = \mu_{out} A_e \Delta \mathbf{u}_{\mathbf{t}}^{\mathbf{e}} / \delta \tag{9}$$

where $\Delta \mathbf{u}^e$ is the velocity difference between external fluid and element e, ρ is the density of external fluid, Q is flow rate passing through element e, μ_{out} is the viscosity of external fluid. δ is equivalent boundary layer thickness which is estimated as $\delta = 4a/9$ based on Stoke's theory. The fluid force on an element is equally distributed to each vertex of that element. The internal force $\mathbf{f}^{\mathbf{in}}$ was modeled in a similar way to $\mathbf{f}^{\mathbf{out}}$.

C. Solving Method

In order to simulate dynamic behavior of an RBC, we solve the motion of each node with mass of m. According to the virtual work principle, the force working on node i due to elastic deformation of an RBC is gained by

$$\mathbf{F}_i = -\frac{\partial W}{\partial \mathbf{r}_i} \tag{10}$$

Given forces acting on node i, the motion of node i is determined from the equation of motion;

$$m\ddot{\mathbf{r}}_i = \mathbf{F}_i + \tilde{\mathbf{f}}_i \quad (11)$$

where a dot means a time derivative.

D. Parameters

Spring constants such as k_b and k_a+k_A and mass m are determined from a comparison with various experiments [11-13]. Deviations of model parameters are described in details in [7]. Used values are: k_A = 4500 μN/m, k_a = 500 μN/m, k_V = 5.0·10^{7}μN/m^2, k_b = 1.0·10^{-4} μN, a = 3.3 μm, μ_{out} = 3.0·10^{-3}Pa·s, μ_{in} = 5.0·10^{-3} Pa·s. To express an increase in stretching resistance with elongation of spectrin, we adopt a spring constant k_s that changes non-linearly as a function of stretching ratio λ;

$$k_s = k_{s0} \exp\{\alpha(\lambda - \beta)\} \quad (12)$$

where α and β are parameter constants. In this study, they were set as α = 2.5, β = 1 by trial and error to achieve the satisfactory match between the simulation and the experiments (see RESULTS B and Fig. 3).

III. Results

A. Determining the initial shape of RBC

Starting with a spherical shape shown in Fig. 1 (a), the volume of RBC was gradually decreased by 40%. With a decrease in the volume, the RBC changed its shape such that the total elastic energy became a minimum while it had a desired volume. The RBC firstly took a cupped (concave) shape at around 80% of the initial volume. However, the RBC became a biconcave shape at 60% of the initial volume. The cross-section of the RBC at the converged state is depicted in Fig. 2. This shape was taken as the natural shape of the RBC hereafter.

B. RBC behaviour in a parallel shear flow

The RBC model was put in the steady parallel shear flow which gives a constant shear γ in the space between two parallel plates, one of which is moving relative to the other. Once the RBC was exposed to the parallel shear flow, it elongated and became ellipsoid. Depending on the magnitude of shear, it tank-treaded, tumbled or did both. The tumbling occurred at the low shear roughly smaller than 20 s^{-1}. As the shear rate γ elevated, the RBC elongated more and started to show tank-treading motion of the membrane. In the present study, a transition from tank-treading to tumbling occurs at the shear rate of 20-40 s^{-1}.

The deformation index L/W is plotted against the external fluid shear stress τ in Fig. 3. Here, L and W are the length of long and short axes of RBC when it is approximated as an ellipsoidal body. The experimental data show that L/W increased linearly until τ=20 Pa and then changed the trend such that L/W converged to a certain value (approximately ~5). The satisfactory match between simulation results and experimental data is achieved when constants in eq. (12) were set as α = 2.5, β = 1.

C. RBC behaviour in a step flow

The RBC behaviour in a step flow with the Reynolds

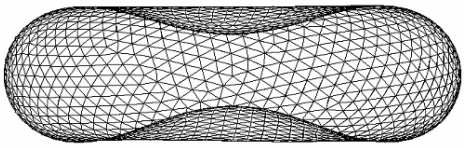

Fig. 2 RBC shape after decreasing the volume by 40%

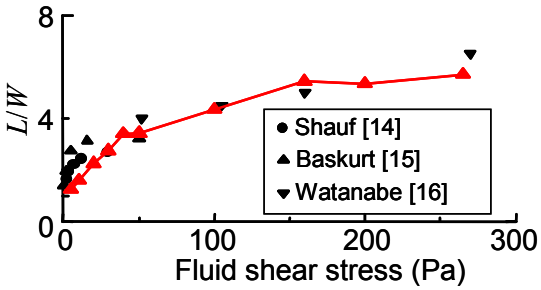

Fig. 3 Relationship between τ and L/W

number of 1000 was simulated. The flow field was obtained by solving the equation of Navier-Stokes along with the equation of continuity by using a commercial software of computational fluid dynamics, STAR-CD (CD-Adapco, Japan) that uses a finite volume method for discretization. Figure 4 depicts the velocity field within the step flow. As seen, the vortex was generated behind the step.

Red dots in Fig. 4 are the trace of RBC that was infused from the inlet. Figure 5 shows the snapshots of an RBC at (A) and (B) which are encircled in blue in Fig. 4. Colour of the RBC in Fig. 5 represents the first principal strain ε. At (A) where flow was comparatively less disturbed, the RBC inclined against the fluid shear and elongated to some extent. It also showed a tank-treading motion, but no tumbling. At this state, a large first principal strain ε was found around the center of RBC. As the RBC flowed downstream and reached the vortex, the RBC started to tumble, although it is not clear from Fig. 5 (B). In this region, the first principal strain ε was not so large as the one observed in (A).

The maximum of the first principal strain over the membrane ε_{max} at each time instant was plotted against *SS* in Fig. 6. *SS* is an index to quantify an instantaneous fluid shear stress tensor at each location, and conventionally used for evaluating haemolysis [4]. As seen in Fig. 6, there was no consistent tendency between the maximum of the first principal strain ε_{max} and *SS*.

IV. Discussion

The simulation results for the steady shear flow showed that the deformation parameter of RBC, L/W, well agreed with experimental results not only in physiological shear stresses (~5 Pa) but also in high shear stresses [14-16]. Those results demonstrate that the present RBC model is capable of expressing realistic deformation behaviour even in a high-shear flow.

The RBC flowing in the back-step flow was exposed to dynamically changing fluid mechanical environment as it

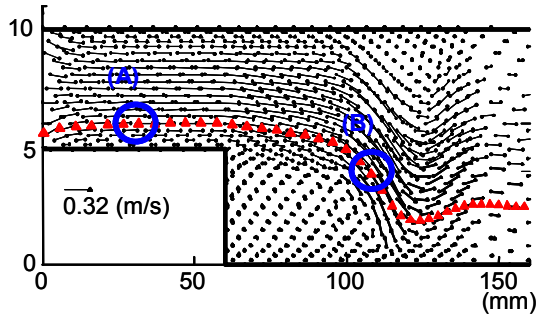

Fig. 4 Vector plots of flow in a back-step flow

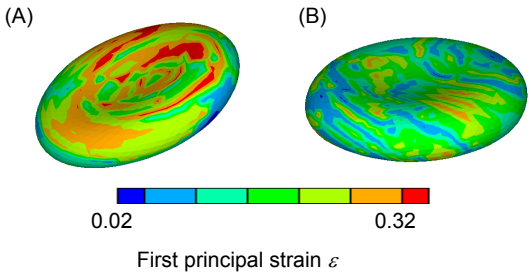

Fig. 5 Snapshots of an RBC in (A), (B)

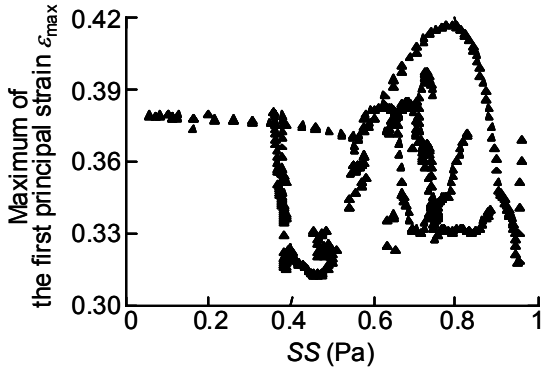

Fig. 6 Relationship between ε_{max} and L/W

moved. Although a viscous property was not considered in the RBC model, the viscous force was generated through the interaction with surrounding fluid forces. As a consequence, the RBC shape was determined not only fluid force acting on it at that moment but also its deformation history.

Quantitative evaluation of hemolysis is essential in designing artificial organs. Recently, numerical methods to quantify hemolysis from a measured or calculated macroscopic flow velocity field have been proposed [4-6]. Nevertheless, their predictive accuracy has not reached a satisfactory level required in practice. As presented in Fig. 6, no consistent tendency was found between the maximum of the first principal strain ε_{max} and haemolysis index *SS*. It means that it is basically impossible to predict the mechanical damage of the RBC membrane solely from a macroscopic flow field. This would be the reason why conventional hemolytic indices have limitations in their accuracy. For amelioration of the predictive accuracy, it would be requisite to take into account motion and dynamical deformation of individual RBCs in a flow field.

V. Conclusion

In conclusion, the results address the necessity to consider dynamic deformation of RBCs for better evaluation of hemolysis. The present model would be useful to build an RBC-based hemolysis simulator.

Acknowledgment

The authors acknowledge Grant-in-Aid for Young Scientists (A) 19680024.

References

[1] R. P. Rother, L. Bell, P. Hillmen, and M. T. Gladwin, "The clinical sequelae of intravascular hemolysis and extracellular plasma hemoglobin: a novel mechanism of human disease," *J. Am. Med. Assoc.,* vol. 293, pp. 1653-1662, 2005.

[2] J. A. Murray, A. Ledlow, J. Launspach, D. Evans, M. Loveday, and J. L. Conklin, "The effects of recombinant human hemoglobin on esophageal motor functions in humans," *Gastroenterology*, vol. 109, pp. 1241-1248, 1995.

[3] A. Schafer, F. Wiesmann, S. Neubauer, M. Eigenthaler, J. Bauersachs, and K. M. Channon, "Rapid regulation of platelet activation in vivo by nitric oxide," *Circulation*, vol. 109, pp. 1819-1822, 2004.

[4] C. Bludszuweit, "Three-dimensional numerical prediction of stress loading of blood particles in a centrifugal pump", *Artif. Organs,* vol. 19, pp. 590-596, 1995.

[5] T. Yano, K. Sekine, A. Mitoh, Y. Mitamura, E. Okamoto, D. W. Kim, I. Nishimura, S. Murabayashi, and R. Yozu, "An estimation method of hemolysis within an axial flow blood pump by computational fluid dynamics analysis," *Artif. Organs,* vol. 27, pp. 920-925, 2003.

[6] L. Wurzinger, R. Opitz, and Eckstein H. "Mechanical blood trauma – an overview," *Angeiologie*, vol. 19, pp. 81-87, 1986.

[7] S. Wada, and R. Kobayashi, "Numerical simulation of various shape changes of a swollen red blood cell by decrease of its volume," *J. Soc. Mech. Eng. Trans. A*, vol. 69, pp. 14-21, 2003 (in Japanese).

[8] J. C. Hansen, R. Skalak, S. Chien, and A. Hoger "An elastic network model based on the structure of the red blood cell membrane skeleton," *Biophys J.*, vol. 70, pp. 146-166, 1996.

[9] S. C. Liu, L. H. Derick, M. A. Duquette, and J. Palek, "Separation of the lipid bilayer from the membrane skeleton during discocyte-echinocyte transformation of human erythrocyte ghosts," *Eur. J. Cell Biol*., vol. 49, pp. 358-365, 1989.

[10] N. Mohandas, and E. Evans, "Mechanical properties of the red cell membrane in relation to molecular structure and genetic defects," *Ann. Rev. Biophys. Biomol. Struct.*, Vol. 23, pp. 787-818, 1994.

[11] E. Evans, and Y. C. Fung, "Improved measurements of the erythrocyte geometry," *Microvasc. Res.*, vol. 4, pp. 335-347, 1972.

[12] R. M. Hochmuth, and R. E. Waugh, "Erythrocyte membrane elasticity and viscosity," *Annu. Rev. Physiol*. vol. 49, pp. 209-219, 1987.

[13] E. A. Evans, R. Waugh, and L. Melnik "Elastic area compressibility modulus of red cell membrane," *Biophys. J*., vol. 16, 585-595, 1976.

[14] B. Schauf, B. Aydeniz, R. Bayer, and D. Wallwiener, "The laser diffractoscope - a new and fast system to analyse red blood cell flexibility with high accuracy," *Lasers Med. Sci*., vol. 18, pp. 45-50, 2003.

[15] O. K. Baskurt, D. Gelmont, and H. J. Meiselman,"Red blood cell deformability in sepsis," *Am. J. Respir. Crit. Care Med.,* vol. 157, pp. 421-427, 1998.

[16] N. Watanabe, H. Kataoka, T. Yasuda, and S. Takatani, "Dynamic deformation and recovery response of a red blood cell to cyclically reversing shear flow: effects of frequency of cyclically reversing shear flow and shear stress level," *Biophys J.*, vol. 91, pp. 1984-1998, 2006.